Novel CineECG Enables Anatomical 3D-Localization and Classification of Bundle Branch Blocks

Machteld J. Boonstra, MSc[1], Bashar N. Hilderink, MD[1], Emanuela T. Locati MD, PhD[2], Folkert W. Asselbergs, MD, PhD[1,3,4], Peter Loh, MD, PhD[1], and Peter M. van Dam, PhD[1,5]

[1] Department of Cardiology, Division Heart & Lungs, University Medical Center Utrecht, The Netherlands;
[2] Department of Arrhythmology and Electrophysiology, IRCCS Policlinico San Donato, Milano, Italy;
[3] Netherlands Heart Institute, Utrecht, The Netherlands;
[4] Institute of Cardiovascular Science and Institute of Health Informatics, Faculty of Population Health Sciences, University College London, London, United Kingdom;
[5] ECG Excellence BV, Nieuwerbrug aan den Rijn, Netherlands.

Word Count: 5080
Figures/tables: 3/2
References: 24

Corresponding Author:
Dr. Peter M van Dam
Division Heart & Lungs, Department of Cardiology,
University Medical Center Utrecht,
3508 GA, Utrecht,
The Netherlands.
Email: peter.van.dam@peacs.nl

Abstract

Background: Ventricular conduction disorders can induce arrhythmias and impair cardiac function. Bundle branch blocks (BBB) are diagnosed by 12-lead ECG, but discrimination between BBBs and normal tracings can be challenging. CineECG computes the temporo-spatial trajectory of activation waveforms in a 3D-heart model from 12-lead ECGs. Recently, in Brugada patients, *CineECG* has localized the terminal components of ventricular depolarization to right ventricle outflow tract (RVOT), coincident with arrhythmogenic substrate localization detected by epicardial electro-anatomical maps. This abnormality was not found in normal or right BBB (RBBB) patients. This study aimed at exploring whether *CineECG* can improve the discrimination between left/right BBB (LBBB/RBBB), and incomplete RBBB (iRBBB).

Methods: We utilized 500 12-lead ECGs from the online Physionet-XL-PTB-Diagnostic ECG Database with a certified ECG diagnosis. The mean temporo-spatial isochrone trajectory was calculated and projected into the anatomical 3D-heart model. We established five *CineECG* classes: "Normal", "iRBBB", "RBBB", "LBBB" and "Undetermined", to which each tracing was allocated. We determined the accuracy of *CineECG* classification with the gold standard diagnosis.

Results: A total of 391 ECGs were analyzed (9 ECGs were excluded for noise) and 240/266 were correctly classified as "normal", 14/17 as "iRBBB", 55/55 as "RBBB", 51/51 as "LBBB" and 31 as "undetermined". The terminal mTSI contained most information about the BBB localization.

Conclusion: CineECG provided the anatomical localization of different BBBs and accurately differentiated between normal, LBBB and RBBB, and iRBBB. *CineECG* may aid clinical diagnostic work-up, potentially contributing to the difficult discrimination between normal, iRBBB and Brugada patients.

Keywords: Electrocardiogram, vectorcardiography, CineECG, Cardiac modeling, ventricular conduction disorders, mean temporal spatial isochrones;

What's new

- *CineECG* provided an automatic and quantitative differentiation between conduction defects by relating ventricular activation to cardiac anatomy of a standard a 3D-heart model.
- *CineECG* provided the anatomical localization of different conduction defects and proved to be a robust method which accurately differentiated between normal, LBBB and RBBB, and iRBBB ECG tracings.
- The terminal part of the mean temporal spatial isochrone trajectory (mTSI) contains most information about the distinct BBB anatomical localization and may specifically contribute to the identification of iRBBB.

Introduction

Normal ventricular activation is mediated through the His-Purkinje system, which rapidly distributes the electrical depolarization wave to the left ventricular (LV) and right ventricular (RV) endocardium. [1-4] The His-bundle system originates at the AV-node and directly divides into several major branches. These major branches divide numerously and terminate in a dense distribution of Purkinje fibers, distributed in a large part of the ventricular endocardium. Conduction defects in one (or more) of these mayor branches regionally delay activation. Ventricular conduction disorders may induce arrhythmias[5] and may impair cardiac function, due to the asynchronous ventricular activation.[6, 7] Intraventricular conduction disorders are typically referred to as bundle branch blocks (BBBs) and are currently identified using the standard 12-lead ECG.

The diagnostic value of the standard 12-lead ECG is limited by the difficulty of linking the ECG data directly to cardiac anatomy. Furthermore, mechanical noise, and inconsistency and variability in electrode positioning may significantly influence recorded ECG waveforms, thereby directly affecting ECG interpretation. [8-10] These factors may contribute to the challenges of the discrimination between BBB and normal tracings. For many decades, the vectorcardiogram (VCG) was thought to overcome these issues as it represents the direction of cardiac activity, either depolarization or repolarization.[11] However, the relation between the VCG and cardiac anatomy remains complex. Therefore, the identification of BBB using the 12-lead ECG remains cumbersome, even for expert ECG-readers.

Complete and incomplete BBB are identified by specific 12-lead ECG waveform characteristics. However, incomplete BBBs may be difficult to detect as the late activated area is relatively small resulting in subtle ECG waveform changes.[12] Moreover, while in the past, incomplete right bundle branch block (iRBBB) and right bundle branch block (RBBB) were typically thought to be benign findings in young adults, more recent studies suggest that they may be associated with severe disease, in both symptomatic and asymptomatic patients.[13] Thus, patients found to have such abnormalities should undergo careful examination to exclude cardiac disease. Furthermore, iRBBB waveform characteristics may resemble non-diagnostic waveform abnormalities detected in patients with suspect Brugada Syndrome (BrS), referred to as type-2 or 3 BrS patterns. Often, even expert cardiologists do not agree on ECG interpretations of BrS patterns, providing inconsistent and discordant diagnostic conclusions.[14] Therefore, the correct identification of iRBBB, is of major clinical relevance.

The *CineECG* method, computes the mean temporo-spatial isochrone (mTSI) trajectory of ECG waveforms and projects this into a 3D-heart model, thereby representing the mean trajectory of the ventricular electrical activation at any time interval related to ventricular anatomy.[15, 16] Recently, in Brugada patients, both with spontaneous or with Ajmaline-induced type-1 pattern, *CineECG* has localized the terminal components of ventricular depolarization to the right ventricle outflow tract (RVOT). This localization coincided with the anatomical arrhythmogenic substrate location detected by epicardial potential-duration maps. This abnormality was not found in normal subjects or in RBBB patients. *CineECG* may be a useful tool to more accurately identify conduction disorders in specific areas of the heart, such as left ventricle (LV), septum or right ventricle (RV), overcoming the challenges of the standard 12-lead ECG interpretation.

This study aimed at exploring whether abnormalities of the mTSI trajectory computed by *CineECG* can allow a simple and precise identification of bundle branch conduction defects, thereby providing a more objective and reproducible discrimination between normal, left BBB (LBBB), right BBB (RBBB), and iRBBB compared to the standard interpretation of the 12-lead ECG.

Methods

CineECG method

CineECG relates electrical cardiac activity to cardiac anatomy by computing the mTSI trajectory. In summary, the mTSI trajectory is derived from the VCG, computed from 12-lead ECG while taking into account the electrode positions on the thorax. Subsequently, a constant conduction velocity is used to project the location of the mTSI trajectory per time interval inside the heart model (**Supplementary Methods**).[17] The mTSI trajectory thus describes the mean direction of all simultaneous ventricular electrical activity during the activation and recovery of the heart, where cardiac activation is related to cardiac anatomy (**Figure 1**). [15, 17] In this study, the MRI-based heart/torso anatomical model of a 58-year-old male with standard electrode positions was used in all cases.[17]The mTSI was computed according to the standard *CineECG* method. [15, 17] The origin of the mTSI trajectory is located in the LV septum. [18]

The root mean square (RMS) curve from all recorded ECG leads was used to identify the onset and end of ventricular activation. Two fiducial points are identified: QRS onset (**Figure 1, white line**) and QRS end (**Figure 1, red line**). The mTSI trajectories were displayed by the standard four-chamber view, the right and left anterior oblique views (**Figure 2**).[18] This enables the quantification of the relation between cardiac anatomy and the mTSI. Establishing the relation between the cardiac anatomy and the (terminal) direction of the mTSI, allows depiction of the region of latest activation during depolarization.

Per recording, one template beat was selected and semi-automatically QRS onset and QRS end were determined (**Figure 1, left panel**). Then, up to eight eligible beats were automatically selected based on similarity of the QRS complex to the template beat (QRS correlation >0.99 and relative difference <0.15). For all selected beats, the mTSI trajectory was computed.

ECG-data and validation of the database

A total of 500 EGCs were utilized from the certified classified Physionet XL PTB Diagnostic ECG Database (500 Hz, https://physionet.org/content/ptb-xl/1.0.1/) (**Table 1**). To comply with the *CineECG* data structure, signals were resampled to 1000 Hz using linear interpolation. ECGs were classified as either no conduction disturbances (normal), incomplete right bundle branch block (iRBBB), complete right bundle branch block (RBBB), complete left bundle branch block (LBBB) or other conduction disturbances. ECGs with other

conduction disturbances (e.g. left anterior fascicular block (LAFB), left posterior fascicular block (LPFB), unspecified intraventricular conduction disturbance (IVCD) or bifascicular blocks) were excluded from analysis.

Due to inconsistencies in the PTB database classification observed prior to the *CineECG* analysis, two trained experts (BH and MB) independently reevaluated all ECG classifications according to the AHA Guidelines.[19] The classifications of BH and MB were combined, inconsistencies identified and consensus was reached from a definitive classification. Compared to the PTB database-classification, a total of 151 ECGs were reclassified. A total of 109 ECGs were excluded from analysis as those were classified as either noise, LAFB, LPFB, IVCD or bifasicular blocks. The definitive classification was used as gold standard.

CineECG parameters

For all 2993 beats from the included 391 ECGs, the following *CineECG* parameters were computed to describe the mTSI trajectory:

3D area: The 3D mTSI area is defined as the area encapsulated by the mTSI trajectory. The QRS area is defined as the area under the X, Y and Z leads which are used to compute the vectorcardiogram. [21]

mTSI location: For each mTSI 1 ms time interval, the mTSI location is determined; e.g. inside the septum, the LV or the RV. The **initial** (first 25 ms), **average** and **terminal** (last 25 ms) location of the mTSI is determined. Each time interval location is labeled to one of the designated areas and displayed as the ratio per area class. During normal activation, a transseptal activation wavefront is expected to be present as activation is first initiated at the LV septum and then moves towards the RV. If the initial trajectory is located more than 10 ms inside the septum, a **transseptal initial vector** is classified as present.

mTSI direction: The main direction is identified as the ratio of activation directed from anterior to posterior, right to left or apex to base with respect to the cardiac anatomy, different from the traditional azimuth and elevation known from VCG analysis which are referenced to the thorax. This ratio is calculated by determining per time interval the direction of the mTSI trajectory. A positive direction indicates movement towards the posterior, left or basal area respectively. A value of zero indicates no movement towards the denoted area. The

more positive or negative the value; the more the mTSI trajectory moves towards, respectively away from the area. The **initial** (first 25 ms), **average** and **terminal** (last 25 ms) mTSI trajectory direction was determined.

Trans-cardiac ratio: The trans-cardiac ratio (**TCR**) is the ratio of the 3D distance between the location of QRS onset and QRS end and heart-model size. [16] The **minimal TCR** is the ratio of the 3D distance between the location of QRS onset and the closest point of the mTSI trajectory to the onset after 60% of the QRS duration and heart-model size.

*Heart axis***:** A **frontal** and **transversal heart axis** were defined by calculating the angle between the left to right axis and a predefined location in the mTSI trajectory. An **initial** (25 ms), **average** and **terminal** (QRS end) location in the mTSI trajectory were computed.

CineECG classification

Relevant *CineECG* parameter and cut-offs were identified using scatter plots, where the relevant parameter (y-axis) was scattered against QRS duration (x-axis). Based on this analysis and a previous study, all beats were classified using the *CineECG* parameters using the following criteria [17]:

1. **Normal**: QRS duration < 110 ms, TCR 2-40%, Terminal-mTSI location RV < 50% and the Terminal Transversal Heart Axis between -100° and 150°.
2. **RBBB**: QRS duration >= 120 ms, TCR > 8%, Terminal-mTSI location RV or Septum > 0. Terminal Transversal Heart Axis <-50° or >50°.
3. **iRBBB** (QRS duration >=100 ms & < 120 ms, minimal TCR < 15%, mTSI location in RV. Terminal Transversal Heart Axis <-75° or >75°.
4. **LBBB**: QRS duration >= 120 ms, TCR > 35%, average transversal HA terminal QRS between 0 and 100, complete mTSI location >70% inside the LV.
5. **Undetermined:** any other value for the above-mentioned *CineECG* parameters.

If in a given ECG, different beats were allocated to different *CineECG* classes, the final *CineECG* class of the complete ECG was determined by identifying the most frequently assigned *CineECG* class over all considered beats.

Statistical analysis

All statistical analysis was performed using MATLAB (2017a). The percentage of correctly classified ECGs was determined as well as sensitivity, specificity, negative predictive value, positive predictive value, accuracy and F1-score were determined per subgroup. Baseline characteristics were tested for statistically significant difference using one-way ANOVA or chi-square tests for continuous respectively categorical variables. A value of $p<0.05$ was considered statistically significant.

Results

The clinical, ECG and *CineECG* characteristics of the 391 cases grouped by their clinical diagnosis are provided in **Table 1**. As can be observed, the age between clinical groups differed significantly (p<0.0001). Furthermore, all *CineECG* derived parameters differed significantly per group (p<0.0001).

mTSI trajectory by each clinical group

The average mTSI trajectories from all 2993 beats per clinical group are shown in **Figure 2**. Per time interval, the average mTSI location was computed (**Figure 2, solid red line**) and the standard deviation was calculated as the mean 3D distance between the average mTSI trajectory and individual mTSI trajectories (**Figure 2, grey tubular envelope**). A clear distinction between normal, RBBB and LBBB activation can be observed. In RBBB activation, the initial part of the mTSI is similar to normal activation whereas in LBBB activation the initial transseptal direction is not present. Differences between iRBBB and normal activation are less pronounced compared to the complete blocks.

Normal activation

In the 266 cases defined on the basis of the 12-lead ECG classification as normal, the mTSI trajectory was compact (**Figure 2**). The initial direction of the mTSI trajectory was mainly transseptal, crossing the septal wall from left to right (**Table 1**). Thereafter, the main direction was towards the middle/basal area of the LV free wall. Overall, the mTSI of the QRS stayed close to or inside the septum and terminated in the LV.

iRBBB activation

In the 17 cases defined as iRBBB, the mTSI trajectory was even more compact compared to the normal mTSI trajectory (**Figure 2**). The first part of the mTSI trajectory is similar to the normal mTSI trajectory. After the initial transseptal movement, the mTSI starts moving towards the apex and back through the septal wall towards the LV. The terminal part points mostly toward the septal wall, indicating late activation in the RV. This compactness was reflected in a lower TCR and minimal TCR and the mTSI location was high for the septum.

RBBB activation

In the 55 cases defined as RBBB, the mTSI trajectory differed from the normal mTSI trajectory in its terminal QRS direction which was directed towards the right basal area (**Figure 2**), reflecting late ventricular activation in this region. Compared to normal TCR, the TCR was increased and increased mTSI location inside the RV was observed. The transseptal vector was less present compared to normal and iRBBB mTSI trajectories (**Table 1**).

LBBB activation

In the majority of the 51 cases defined as LBBB, a transseptal vector was absent in the mTSI trajectory. In these subjects, the mTSI moved from the LV septal wall towards the LV free wall, which was reflected in the mTSI location. The terminal mTSI of the QRS was directed to the LV free wall (b), with a large TCR (**Table 1**), the mTSI was never located in the RV, and a transseptal vector was less present (**Table 1**).

CineECG classification output

All 2993 beats (from 391 ECGs) were classified according to the *CineECG* criteria as either "normal", "iRBBB", "RBBB", "LBBB" or "undetermined" and these classifications were used to determine the definitive *CineECG* class per ECG. Two-dimensional scatterplots were used to determine the relevancy and cut-off values per *CineECG* parameter (**Figure 3A**). In 41 ECGs, beats of one ECG were assigned to two or more CineECG classes, either to the "normal", "iRBBB" or "undetermined" group and thereof 27 ECGs were classified correctly. **Table 2** shows the detailed diagnostic performance of the *CineECG* classification for the different clinical groups. A high performance was obtained for normal, RBBB and LBBB groups. For iRBBB activation, sensitivity was lower compared to the other groups. For RBBB and LBBB groups, the *CineECG* classification and the clinical diagnosis were always coincident (**Figure 3B**). Vice versa, less consistency between *CineECG* and clinical diagnosis was observed in discriminating between iRBBB from normal, especially in beats with a QRS duration between 100 and 110 ms.

Discussion

This is the first study utilizing *CineECG* to characterize ventricular activation defects and classify BBB by using 3-D anatomical characteristics of the mTSI trajectory. Using *CineECG* criteria, all RBBB and LBBB tracings, and most IRBB and normal tracings, were classified correctly in accordance with standard 12-lead clinical classification. *CineECG* provides an easy to use tool to obtain a comprehensive insight into the relation between ventricular activation and anatomy and is therefore helpful for clinicians to accurately discriminate between different conduction disorders. However, between iRBBB and normal activation, overlap exists between the clinical groups, particularly between 100 and 120 ms QRS duration. A clear distinction between the types of blocks can be visually observed in the average mTSI trajectories (**Figure 2**). The terminal vector of the mTSI trajectory points towards the area of latest activation, thereby indicating the location of the block. However, the differentiation between an iRBBB and a normal pattern remains challenging and requires further optimization.

The relation between mTSI and BBB location

The average mTSI trajectories observed in this study, clearly show distinct patterns for different types of BBB (**Figure 2**). For the complete BBB, a clearly deviating pattern from the normal can be observed. While in LBBB activation patterns, the mTSI trajectory mainly moves leftwards and inside the LV cavity, in RBBB activation patterns, the mTSI trajectory initially moves toward the LV cavity whereafter it moves towards the RV basal area (**Figure 2**). Thus, while the mTSI trajectory of LBBB solely moves leftwards, the mTSI trajectory for RBBB starts leftwards, and then goes rightwards. This may be explained by the larger amount of LV myocardial mass, with respect to the RV myocardial mass, and thus LV activation is likely to conceal activation occurring in the RV. Since *CineECG* takes cardiac anatomy into account, mTSI trajectories might be viewed as a more reliable alternative to identifying BBB than the current ECG strict criteria for LBBB and RBBB, also considering inter-individual age and gender variation. [6, 12]

Clinical classification of iRBBB

QRS duration is one of the main clinical characteristics to differentiate between normal, incomplete, and complete RBBB. An iRBBB is identified when QRS-duration ranges between 110 and 120 ms, but may be wrongly classified in cases of incorrect manual or machine interpretation of the 12-lead ECG, further

magnified due to inter-lead QRS duration differences. Therefore, a coherent way to measure the QRS duration is of utmost importance in order to correctly differentiate between normal and iRBBB activation. *CineECG* is likely to overcome these difficulties. In case of iRBBB, the mTSI trajectory is compact and stays within the septum and clearly differs from both normal and RBBB activation (**Figure 2**). Thus, 1) the temporo-spatial location of the mTSI trajectory contains all information about the direction and timing of ventricular depolarization, and 2) the mTSI terminal direction indicates the anatomical location of the block, by pointing towards the latest site of activation. With increasing QRS duration in iRBBB cases, a clear shift of the terminal mTSI direction towards the RV base was observed, becoming more similar to the RBBB mTSI trajectory (**Figure 2**).

Comparison to standard 12-lead ECG assessment

In this study, we validated our *CineECG* method with the clinical 12-lead ECG assessment. However, ultimately, the comparison of *CineECG* classification to standard 12-lead ECG clinical assessment through invasive electro-anatomical activation mapping should be performed. Through invasive mapping, the true location of the BBB may be identified and the ability of *CineECG* and standard clinical 12-lead to identify these BBBs correctly can then be assessed.

Starting point mTSI trajectory

In *CineECG*, the starting point of the mTSI trajectory was set at the left side of the septal wall closest to the ventricular center of mass. During normal activation, a transseptal wavefront of activation moves from the LV side of the septum towards the right. However, in LBBB cases the transseptal vector is reversed and thus classified as not present in 53% (**Table 1**). Therefore, this starting point may inadequately represent the true start of LBBB activation, as such activation starts at the RV septum or RV free wall. Furthermore, due to intra-individual differences in bundle branch anatomy, this starting point may inadequately represent the true starting point of ventricular activation. The starting point therefore serves as a general starting point, but as shown in this study, *CineECG* provides an accurate concise way to assess average ventricular activation related into cardiac anatomy, where the starting point does not yet seem to be a constraint for the *CineECG* classification.

Limitations

The use of a standardized heart torso model, rather than a personalized model, may limit the accuracy of the presented results. The use of the standard torso/heart model enables the direct projection of the mTSI to the cardiac anatomy, but differences in heart anatomy and orientation, thorax anatomy and lead position are not accounted for. With age, the shape, position and orientation of the heart in the torso may change. In this study, we used a standard anatomical heart/torso model based on a 58-year-old male, which may adequately represent adult RBBB and LBBB male cases (**Table 1**) but may be inadequate for the younger iRBBB and normal cases and more generally, for female cases. Using a standardized heart/torso model may result in a larger *CineECG* parameter variation, caused by intra-individual variation in cardiac anatomy. Thus, the distribution of mTSI derived parameters per BBB group encompass larger standard deviations as activation is referenced to a cardiac anatomy with an incorrect size, shape and/or orientation, also relative to the thoracic model and electrode locations. Therefore, using a 3D camera to localize the ECG electrodes and the torso dimensions might increase the accuracy of our method. [22, 23,24] These factors may be particularly relevant for the more accurate identification of iRBBB.

In PTB database, the number of IRBB cases was very small. Besides, we found some inconsistencies in the PTB database classification, particularly regarding iRBBB cases. Therefore, we revised all the included ECG and upon agreement of two independent experts we came to a definitive classification, of the PTB tracings which we used for the statistical analysis. Given the clinical relevance of analysis of the late depolarization signals, we plan to perform a prospective study studying *CineECG* characteristics of patients with different intraventricular conduction disorders.

Future perspectives

Ambiguity in the standard 12-lead ECG classification can be caused by the presence of intra-individual differences in cardiac anatomy (size, shape), cardiac orientation (due to age, effects of breathing, thoracic shape), bundle branch anatomy, the presence of cardiac disease (scar, myocarditis, fibrofatty tissue) and inconsistency in the placement of electrodes relative to the heart. All these factors may contribute to determine the ECG waveform morphology and 12-lead ECG diagnostic criteria of BBB may be present in the 12-lead ECG in the absence of a true BBB. Through *CineECG*, a more comprehensive view is given on the cardiac

electrical activity using the 12-lead ECG, thereby providing a tool less prone to intra-individual characteristics. Further testing and optimization of this technique is still required. For example, the effect of the presence of scar or ischemia, or more generally myocardial structural diseases, should be assessed in future studies. Furthermore, the ability of *CineECG* to correctly discriminate between iRBBB, RBBB, LBBB, unspecified intraventricular conduction disorders and left anterior and posterior hemiblocks, or even the coexistence of these conduction disturbances should be assessed.

Conclusions

The advanced interpretation of the 12-lead ECG through the *CineECG* method proved to be a robust technique to differentiate between different intraventricular bundle branch conduction defects. The mTSI trajectory relates cardiac activation to cardiac anatomy, thereby directly identifying the anatomical location of the BBB, mostly indicated by the terminal part of the mTSI trajectory. The *CineECG* classification was able to accurately discriminate between normal, RBBB and LBBB cases. Further optimization of the classification algorithm may enhance the *CineECG* classification of iRBBB. The *CineECG* method, directly derived from 12-lead ECG, can be viewed as a noninvasive mapping tool and may improve the early recognition and the monitoring of the progression of intraventricular bundle branch conduction defects.

Acknowledgement

Conflict of Interest

Peter van Dam is one of the owners of ECG Excellence.

Abbreviations

- **BBB** = Bundle Branch Block
- **ECG =** Electrocardiogram
- **iECG =** Inverse electrocardiogram
- **iRBBB** = Incomplete right bundle branch block
- **LBBB** = Left bundle branch block
- **LV =** Left Ventricle
- **RBBB** = Right bundle branch block
- **RV =** Right ventricle
- **mTSI** = mean temporal spatial isochrone

Figure legends

Figure 1 – The computation of the mean temporal spatial isochrone (mTSI) trajectory. First, the standard 12-lead electrocardiogram (ECG, left box) is used to compute the vectorcardiogram. Subsequently the mTSI locations are computed with starting point at the center of the ventricular mass projected into the LV septum (right box, arrow starting point) by taking into account electrode positions and the anatomical location of the heart. The mTSI trajectory is constructed as the 3D location of activation per millisecond moving with a velocity of 0.7 m/s. The QRS complex is segmented using the white and red line. These colors correspond to the colors in the vectorcardiogram and mTSI trajectory, which is displayed in two-dimensional view and three-dimensional view (3D *CineECG* view). Trajectories are either displayed in the four-chamber view (4-chamber), the left anterior oblique view (LAO), the right anterior oblique view (RAO) or the anterior posterior view (AP).

Figure 2 – The average *CineECG* mTSI trajectories according to ECG diagnosis. For all four groups: normal, incomplete right bundle branch block (iRBBB), right bundle branch block (RBBB) and left bundle branch block (LBBB), mTSI trajectories are displayed in the four-chamber view (left column) and apical view (right column). The standard deviation around the average mTSI trajectory is indicated by the black tubular envelope and the mean mTSI direction is indicated in red.

Figure 3A – Setting the *CineECG* BBB classification criteria. A representative example of a two-dimensional scatterplot of all selected beats where the mTSI location parameter is scattered against QRS duration (x-axis). The dots in all plots designate measured mTSI location per beat plotted as a function of QRS duration, classified as either normal (blue), incomplete right bundle branch block (iRBBB, green), right bundle branch block (RBBB, black) or left bundle branch block (LBBB, red). As can be observed for LBBB, the mTSI location is most of the time located inside the left ventricular cavity and never in the right ventricular cavity, whereas for RBBB it is mainly located inside the right ventricular cavity. Such two-dimensional scatterplots were used to identify the relevancy and cut-off values of *CineECG* parameters. Mentioned *CineECG* criteria were set by a combination of data obtained in a previous study [17] and observations made in the current study.
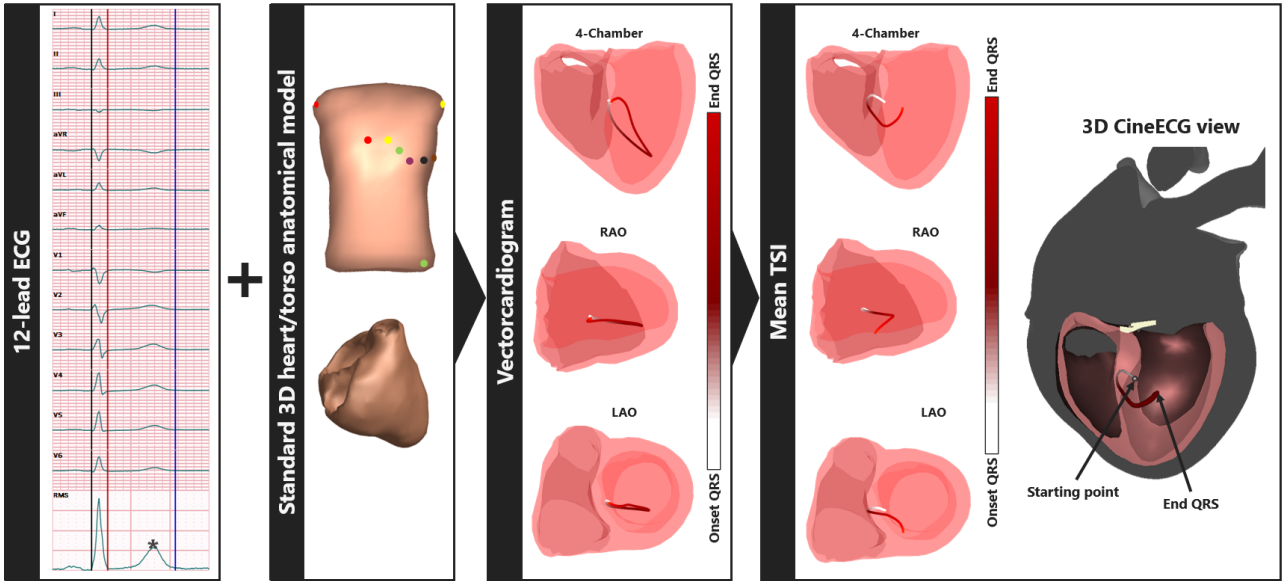
Figure 3B – ***CineECG* BBB Classification** The beat adjudication according to the *CineECG* criteria (x-axis) against QRS duration (y-axis) to show overlap between QRS duration but were assignment to a different group. Colors of the dots indicate the clinical group. The dots in all plots indicate measured values per beat plotted as a function of QRS duration, diagnosed as either normal (blue), right bundle branch block (iRBBB, black), incomplete RBBB (green) or left bundle branch block (LBBB, red).

1

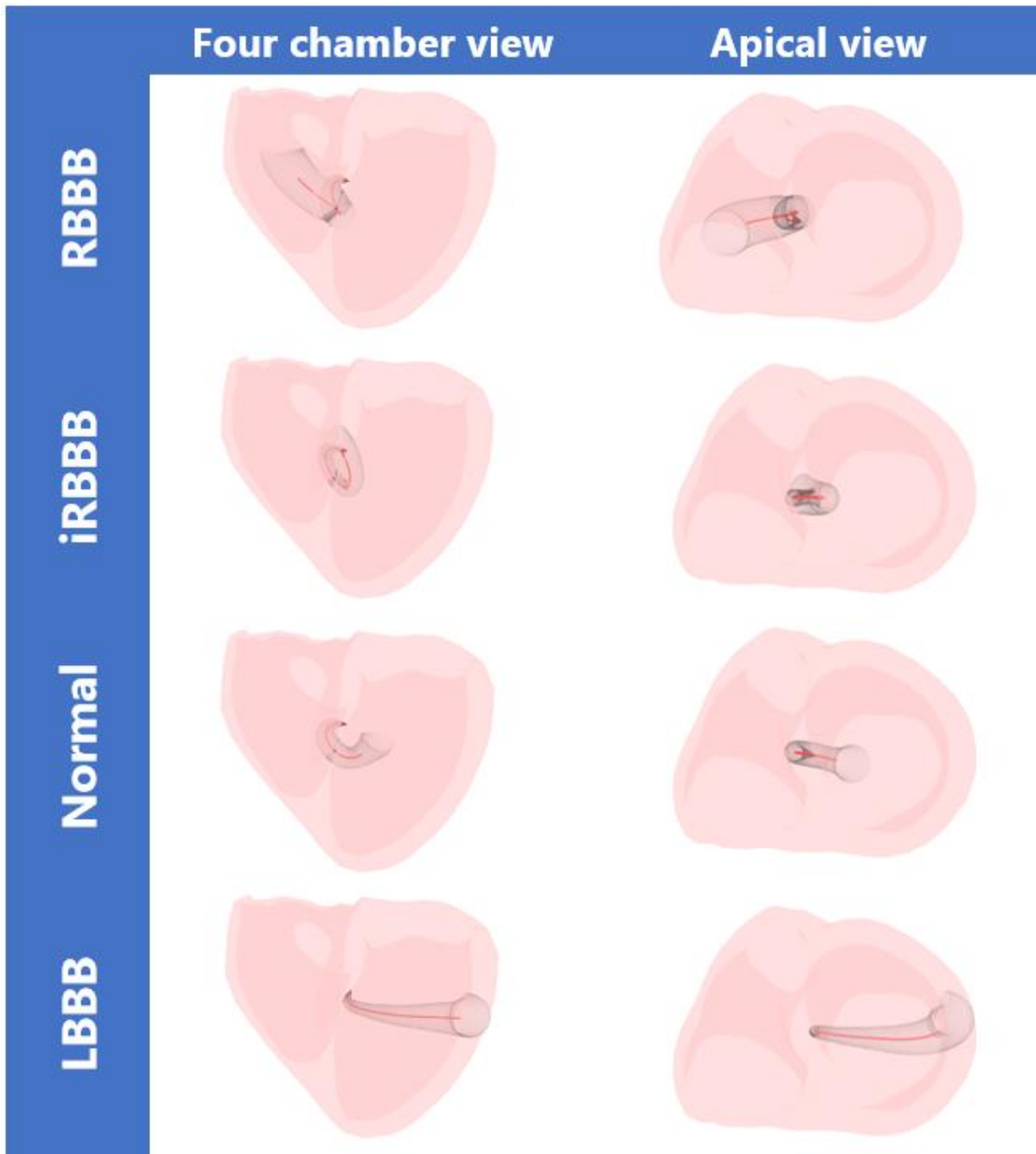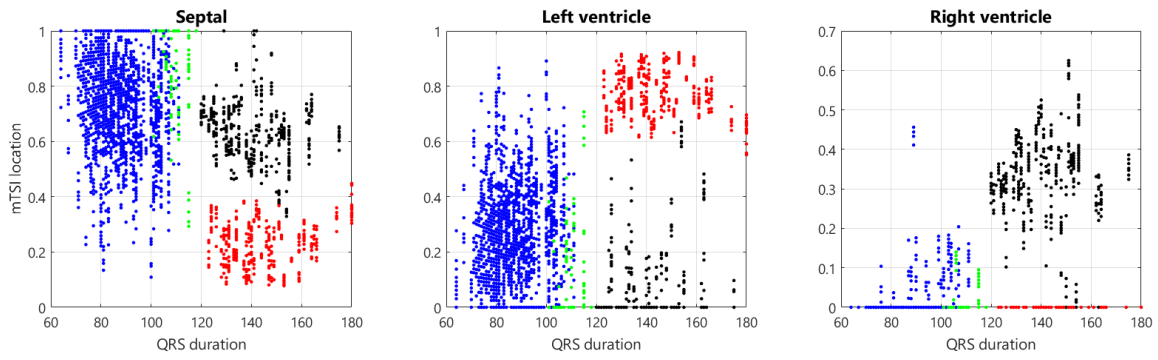**Figure 1 – CineECG method**

3

4

5

6

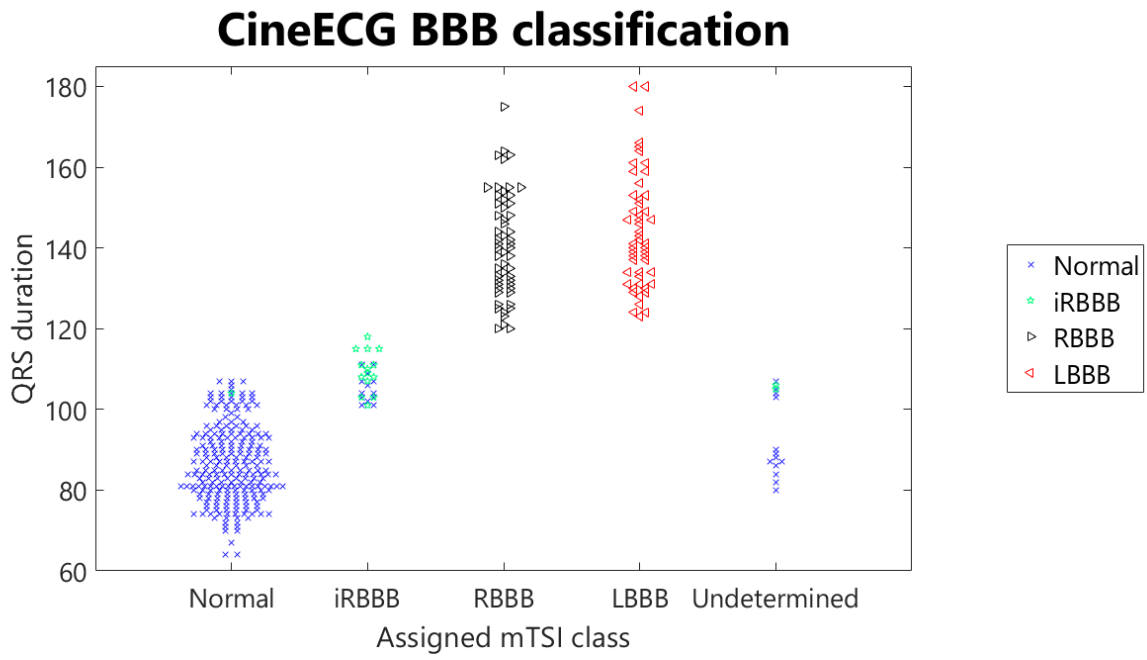1   **Figure 2 – Average mTSI trajectories per clinical group**

2

3

1   **Figure 3A – Setting the *CineECG* BBB classification criteria**

2

1   **Figure 3B – *CineECG* BBB Classification.**

2

CineECG BBB classification

3

1 **Table 1 –** The clinical, electrocardiographic and *CineECG* characteristics of the 391 cases grouped by their clinical diagnosis.

	Normal	iRBBB	RBBB	LBBB	P
Clinical characteristics					
Cases (n)	266	17	55	51	
Beats (n)	2065	126	409	393	
Age (years)	47±19	47±20	69±14	74±9	<0.0001
Gender (% male)	54%	35%	42%	59%	0.132
CineECG characteristics					
QRS duration (ms)	87±10	108±5	141±13	144±14	<0.0001
QT duration (ms)	395 ±34	411 ±42	439 ±58	431±54	<0.0001
TCR (%)	21 ±9	18 ± 8	41 ± 9	48 ± 4	<0.0001
Minimal TCR (%)	18 ± 10	11 ± 9	21 ± 15	48 ± 4	<0.0001
Transseptal vector present (%)	95	97	87	47	<0.0001
Angle transseptal initial vector (%)	129±28	134±23	123±30	82±37	<0.0001

2 *Values are displayed as mean ± standard deviation, a p-value <0.05 was considered statistically significant. Abbreviations: iRBBB = incomplete*
3 *right bundle branch block, RBBB = right bundle branch block, LBBB = left bundle branch block, QRS = QRS complex, QT = Q-wave to end T-wave,*
4 *TCR = trans cardiac ratio.*

5

6 **Table 2 –** The overall performance of the CineECG classification scheme for the classification of ECGs.

	Normal	iRBBB	RBBB	LBBB
Sensitivity	90.2	82.4	100	100
Specificity	99.2	96.5	100	100
Negative predictive value	82.4	99.2	100	100
Positive predictive value	99.6	51.9	100	100
Accuracy	94.7	63.6	100	100
F1-score	93.1	95.9	100	100

7 *Values are displayed as percentages. Ranges of confidence intervals were equal to the mean presented in this table. Abbreviations: iRBBB =*
8 *incomplete right bundle branch block, RBBB = right bundle branch block, LBBB = left bundle branch block*

References

1.	Tawara S. Das Reizleitungssystem des Säugetierherzens. Eine Anatomisch-Histologische Studie über das Atrioventrikularbündel und die Purkinjeschen Faden. Jena: Gustav Fischer; 1906.

2.	Tawara S. Die Topographie und Histologie der Bruckenfasern. Ein Beitrag zur Lehre von der Bedeutung der Purkinjeschen faden. . Zentralb Physiol 1906;19:70–76.

3.	Demoulin J and Kulbertus H. Histopathological examination of concept of left hemiblock. British Heart Journal. 1972;34:807.

4.	Oosthoek PW, Viragh S, Lamers WH and Moorman AF. Immunohistochemical delineation of the conduction system. II: The atrioventricular node and Purkinje fibers. Circulation Research. 1993;73:482-491.

5.	Kusumoto FM, Schoenfeld MH, Barrett C, Edgerton JR, Ellenbogen KA, Gold MR, Goldschlager NF, Hamilton RM, Joglar JA, Kim RJ, Lee R, Marine JE, McLeod CJ, Oken KR, Patton KK, Pellegrini CN, Selzman KA, Thompson A and Varosy PD. 2018 ACC/AHA/HRS Guideline on the Evaluation and Management of Patients With Bradycardia and Cardiac Conduction Delay: A Report of the American College of Cardiology/American Heart Association Task Force on Clinical Practice Guidelines and the Heart Rhythm Society. Circulation. 2019;140:e382-e482.

6.	Strauss DG, Selvester RH and Wagner GS. Defining left bundle branch block in the era of cardiac resynchronization therapy. Am J Cardiol. 2011;107:927-34.

7.	Vassallo JA, Cassidy DM, Marchlinski FE, Buxton AE, Waxman HL, Doherty JU and Josephson ME. Endocardial activation of left bundle branch block. Circulation. 1984;69:914-23.

8.	Drew BJ and Adams MG. Clinical consequences of ST-segment changes caused by body position mimicking transient myocardial ischemia: hazards of ST-segment monitoring? J Electrocardiol. 2001;34:261-4.

9.	Macfarlane PW, Colaco R, Stevens K, Reay P, Beckett C and Aitchison T. Precordial electrode placement in women. Neth Heart J. 2003;11:118-122.

10.	Bond RR, Finlay DD, Nugent CD, Breen C, Guldenring D and Daly MJ. The effects of electrode misplacement on clinicians; interpretation of the standard 12-lead electrocardiogram. European Journal of Internal Medicine. 2012;23:610-615.

11.	Frank E. General Theory of Heart-Vector Projection. Circulation Research. 1954;2:258-270.

12.	Galeotti L, van Dam PM, Loring Z, Chan D and Strauss DG. Evaluating strict and conventional left bundle branch block criteria using electrocardiographic simulations. Europace. 2013;15:1816-21.

13.	Nasir JM, Shah A and Jones S. THE SIGNIFICANCE OF INCOMPLETE AND COMPLETE RIGHT BUNDLE BRANCH BLOCKS IN YOUNG ADULTS. Journal of the American College of Cardiology. 2012;59:E1939.

14.	Chevallier S, Forclaz A, Tenkorang J, Ahmad Y, Faouzi M, Graf D, Schlaepfer J and Pruvot E. New Electrocardiographic Criteria for Discriminating Between Brugada Types 2 and 3 Patterns and Incomplete Right Bundle Branch Block. Journal of the American College of Cardiology. 2011;58:2290-2298.

15.	van Dam PM. A new anatomical view on the vector cardiogram: The mean temporal-spatial isochrones. J Electrocardiol. 2017;50:732-738.

16.	Roudijk R, Loh KP and van Dam PM. Mean Temporal Spatial Isochrones Direction as Marker for Activation Delay in Patients with Arrhythmogenic Cardiomyopathy. Computing in Cardiology. 2018;45:1-4.

17.	van Dam PM, Locati ET, Ciconte G, Borrelli V, Heilbron F, Santinelli V, Vicedomini G, Monasky MM, Micaglio E and Giannelli L. Novel CineECG Derived from Standard 12-Lead ECG Enables Right Ventricle Outflow Tract Localization of Electrical Substrate in Patients with Brugada Syndrome. Circulation: Arrhythmia and Electrophysiology. 2020;13:e008524.

18.	Durrer D, van Dam RT, Freud GE, Janse MJ, Meijler FL and Arzbaecher RC. Total excitation of the isolated human heart. Circulation. 1970;41:899-912.

19.	Surawicz B, Childers R, Deal BJ and Gettes LS. AHA/ACCF/HRS Recommendations for the Standardization and Interpretation of the Electrocardiogram: Part III: Intraventricular Conduction Disturbances: A Scientific Statement From the American Heart Association Electrocardiography and Arrhythmias Committee, Council on Clinical Cardiology; the American College of Cardiology Foundation; and the Heart Rhythm Society: Endorsed by the International Society for Computerized Electrocardiology. Circulation. 2009;119:e235-e240.

20.	Kors JA, van Herpen G, Sittig AC and van Bemmel JH. Reconstruction of the Frank vectorcardiogram from standard electrographic leads: diagnostic comparison of different methods. Eur Heart J. 1990;11:1083-1092.

21.	van Stipdonk AM, Ter Horst I, Kloosterman M, Engels EB, Rienstra M, Crijns HJ, Vos MA, van Gelder IC, Prinzen FW and Meine M. QRS area is a strong determinant of outcome in cardiac resynchronization therapy. Circulation: Arrhythmia and Electrophysiology. 2018;11:e006497.

22.   van Dam PM, Gordon JP and Laks M. Sensitivity of CIPS-computed PVC location to measurement errors in ECG electrode position: the need for the 3D camera. J Electrocardiol. 2014;47:788-93.

23.   Alioui S, Kastelein M, EM vD and PM vD. Automatic Registration of 3D Camera Recording to Model for Leads Localization. Computing in Cardiology. 2017;44:4.

24.   van Dam PM, Boyle NG, Laks MM and Tung R. Localization of premature ventricular contractions from the papillary muscles using the standard 12-lead electrocardiogram: a feasibility study using a novel cardiac isochrone positioning system. Europace. 2016;18:iv16-iv22.